Supplementary Information

Structural Ordering Driven Enhancement of Electrical Conductivity and Mechanical Performance in PEDOT: PSS via Sustainable Additives for Flexible Electronics

*Branston E. Mefferd, [a, †] Ashutosh Shrivastava, [a, †] Visakhan V. Nambiar,[b, †] Yutika R. Badhe,[c] Srikar, V. Charmarthi, [a] Allen Liang, [a] Walter E. Voit,[c] Hongbing Lu,[b] Mihaela C. Stefan [a, *]*

[a] Department of Chemistry and Biochemistry, School of Natural Sciences and Mathematics, The University of Texas at Dallas, 800 W Campbell Rd, Richardson, TX 75080.

[b] Department of Mechanical Engineering, Erik Jonsson School of Engineering and Computer Science, The University of Texas at Dallas, 800 W Campbell Rd, Richardson, TX 75080

[c] Department of Materials Science & Engineering, Erik Jonsson School of Engineering and Computer Science, The University of Texas at Dallas, 800 W Campbell Rd, Richardson, TX 75080

Table of Contents:

EXPERIMENTAL SECTION

Chemicals and Materials

PEDOT: PSS PH1000 (Ossila), Nylon filter sheets (1.0 μm pore size, Tisch Scientific), Sylgard 184 Silicone elastomer (PDMS, DOW Chemical Company), PET sheets (Sigma-Aldrich), glass slides (Fisher), dimethyl sulfoxide (DMSO, TCI America), ethylene glycol (EG, Sigma-Aldrich), tetrahydrofuran (THF, Fisher Chemical), methanol (MeOH, Fisher chemical), Cyrene™ (Sigma-Aldrich), 2-methyl tetrahydrofuran (2-MeTHF, Sigma-Aldrich), ethanol (EtOH, Fisher Chemical), glycerol (TCI America), citric acid (Fisher Chemical), D-sorbitol (Ambeed), erythritol (Ambeed), ascorbic acid (Asc. Acid, Sigma-Aldrich), silver epoxy (Creative Materials), one part epoxy (MED-OG116-31, Epoxy Technology), cables (Cooner Wires), pins (Phoenix Enterprises), acetone (Fisher Chemical), isopropyl alcohol (IPA, Fisher chemical) were all used as received.

Preparation of PEDOT: PSS Films

PEDOT: PSS solvent additive films were prepared in 5% volume ratio. PEDOT: PSS solid additive films were prepared in a 1%W/W ratio to the solution weight. Square glass slides (19 × 19 mm) and PET strips cut from the original sheet (5 × 50 mm and 25 × 20 mm) were cleaned in deionized (DI) water mixed with detergent, DI water, acetone, and IPA, followed by drying under N_2 gas. 600 μL of the respective PEDOT: PSS solution was drop-cast onto a glass slide and air-dried overnight. The films were then annealed for 15 minutes at 90 °C and 15 minutes at 110 °C. Glycerol-treated films showed solvent droplets on the surface after this process and thus were further annealed for 15 minutes at 160 °C to remove the remaining solvent. These films were used for nanoindentation, conductivity, powder X-ray diffraction, Raman infrared, surface profiling, thermal analysis, and thickness measurements. Films for the peel tests were prepared by first gluing a 25 × 20 mm PET strip to the top of a microscope slide. This was then treated with UV-ozone for 30 minutes. From here, 600 μL of the respective PEDOT: PSS solutions were drop cast onto the PET and heated on a hotplate at 80 °C until some corners solidified. At this point, nylon filters were cut into 2.5 × 10 cm strips, placed on top of the solution, and allowed to dry following an analogous annealing cycle to the films cast on glass slides. Cyclic bending samples were prepared by placing 5 × 50 mm PET strips onto a 10 × 13 cm glass slide lined with double-sided tape. This was then treated for 30 minutes with UV-Ozone, and 400 μL of the respective PEDOT:

PSS was drop cast onto the PET strips and allowed to air dry overnight. Afterward, the films were annealed under the same conditions as the glass slide and peel test films. From here, two drops of silver epoxy were applied roughly 3.0 cm from one another and cured at 150 °C for 10 minutes before cooling in air to room temperature. PDMS was prepared in a 10:1 (elastomer: cross-linker) ratio and coated with a blade along the glass slide to form a smooth, even encapsulation layer over the PEDOT: PSS. The PDMS was cured at room temperature for 48 hours before removing the layer from the silver connections. Additional silver epoxy was applied to the connections, and low-resistance wires attached to pins through soldering were placed inside the uncured epoxy. These were then annealed at 150 °C for 15 minutes before being allowed to cool in air to room temperature. Upon complete cure, a one-part epoxy was applied over the connections and UV-cured for 5 minutes under UVA irradiation (315 – 400 nm). The films were removed from the glass slide with a razor blade and subjected to cyclic bending while monitoring the resistance.

Characterization Techniques

Thermogravimetric analysis (TGA, SDT-Q600 TA) was conducted under atmospheric conditions at a heating rate of 10 °C/minute from room temperature to 600 °C.

Nanoindentation was carried out on an Agilent G200 system at room temperature. The G200 has a maximum depth of >500 μm and a maximum load of 500 mN with a resolution of ±50 nN and <0.01 nm, respectively. Before each nanoindentation measurement, the instrument and films were allowed to equilibrate to minimize thermal drift, which had a maximum allowable rate of 0.05 nm/s. Nanoindentation was carried out to a maximum load of 2.0 mN over 200 s, at a loading rate of 0.01 mN/s for all samples. Throughout a 200-second nanoindentation test, the maximum drift was determined to be ±10 nm, corresponding to less than 2% of the maximum nanoindentation depth in the film with the shallowest nanoindent. All the nanoindentation experiments were conducted in a 3 × 3 grid pattern for statistics. The indentation depth for all the samples is less than 10% of the sample thickness. The load displacement curve is provided in Figure 4 (a and d) and Table S2.

Film thickness was measured using a mechanical profilometer (XP-1 Ambios Technology) with a stylus force of 0.05 mg over a scan length of 1.5 mm at a rate of 0.05 mm/s. Three measurements were taken across a cut that spanned the length of the films to ensure uniform thickness. Surface

profiles and roughness were measured via laser-confocal microscopy (Keyence 3D Surface Profiler VK-X Series, λ = 408 nm) with a 0.4 μm radius laser beam. Film thickness and Roughness data are given in Table S2.

Viscoelastic Analysis Procedure

This method was developed by Lu et al for linearly viscoelastic indentation of time-dependent materials.[1] In this study, a Berkovich indenter tip was used, and we consider the indentation of a homogeneous, isotropic, linearly viscoelastic half-space under a constant loading rate, where the load is given by $P(t) = v_0 t H(t)$, with v_0 being the loading rate and $H(t)$ the Heaviside unit step function. Utilizing the generalized Kelvin model and applying these conditions, the indentation displacement, $h(t)$, can be represented as,

$$h^2(t) = \frac{(1-v)v_0 tan\alpha}{4}\left[\left(J_0 + \sum_{i=1}^{N} J_i\right)P(t) - \sum_{i=1}^{N} J_i(v_0\tau_i)\left(1 - e^{\frac{P(t)}{v_0\tau_i}}\right)\right] \quad \text{(S4)}$$

where v is Poisson's ratio, which is 0.33 (based on previous studies)[5] for PEDOT: PSS, α is the angle between the cone generator and substrate plane, J_0 and J_i (in this study, i =1,2,3) are shear creep coefficients, and τ_i are retardation times.[2, 3] Equation S1 is used to fit the data from the load-displacement curves acquired through experiment in order to determine shear creep coefficients. The creep function of the generalized Kelvin model is given in the Prony series below.

$$J(t) = J_0 + \sum_{i=1}^{N} J_i\left(1 - e^{-\frac{t}{\tau_i}}\right) \quad \text{(S5)}$$

where $J(t)$ is the shear creep compliance function. Through the use of a numerical interconversion utilizing a MATLAB code, the shear relaxation function based upon the generalized Maxwell model is determined.[4]

$$\mu(t) = \mu_\infty + \sum_{i=1}^{N} \mu_i e^{-\frac{t}{\lambda_i}} \quad \text{(S6)}$$

where μ(t) is the shear relaxation function, μ_∞ and μ_i (i = 1,2,3) are shear relaxation coefficients, and λ_i are relaxation times. The equilibrium shear relaxation modulus, μ_∞, is considered to be the shear modulus, and the elastic modulus is determined by the relation,

$$E_\infty = 2\mu_\infty(1 + \nu) \tag{S7}$$

where E_∞ is considered to be the elastic modulus.

Error analysis:

The modulus used for comparison between the films is calculated from the nanoindentation load-displacement curves using viscoelastic contact analysis for each indent per film. For each film, the average modulus and standard deviation are calculated from 8 indents, as shown in Table 3 and Figure 5.

Powder X-ray diffraction (PXRD, Bruker D8 Advance diffractometer) was collected with a Cu radiation source (Cu K-α, λ = 0.154 nm) and Lynxeye XE detector using a low background sample holder from 2θ: 2° to 30° with a step size of 0.02°. The data was processed with the diffract.Eva software to get the background-subtracted data, which were plotted as shown in Figure 3. The d-spacing corresponding to the 2θ was calculated based on Cu K-α, λ = 0.154060 nm, and the order of reflection is 1.

Resistance measurements were taken with a Keithley 2400 source meter, and conductivity was calculated as follows:

$$R_s = R \times \frac{\pi}{ln2} \tag{S1}$$

where R_s is the sheet resistance, and R is the measured resistance. The sheet resistance was converted to resistivity through the following relationship,

$$\rho = R_s \times t \tag{S2}$$

where ρ is the resistivity (Ω cm), and t is the film thickness (cm). Finally, conductivity (S/cm) is calculated by taking the inverse of resistivity,

$$S = \frac{1}{\rho} \tag{S3}$$

Raman infrared spectroscopy (Horiba, LabRAM Soleil) utilized a 532 nm laser at 18 mW (20% power) under low-frequency laser mode.

180° peel tests were conducted on a tensile tester (Instron, 500 N load cell) at a 50 mm/min displacement rate until the films reached failure.

PEDOT: PSS contact angles were measured on a PET substrate treated with UV-ozone for 30 minutes using a drop volume of 2.0 μL with a goniometer (Rame-Hart Model 250). Standard deviation was calculated from two experiments on a film for each sample.

Bending tests were performed on a custom-made apparatus, and resistance was monitored using a 2400 Keithley source meter. The bending setup utilizes 3D-printed components mounted on two servo motors positioned opposite each other. These motors rotate in synchronization, enabling a coordinated bending motion that allows for precise testing of material flexibility at a predefined frequency. The entire system was programmed using an Arduino Uno microcontroller, which enabled precise control of the movement.

Note: all tables containing a “percent change” or “multiplicative increase in conductivity” column

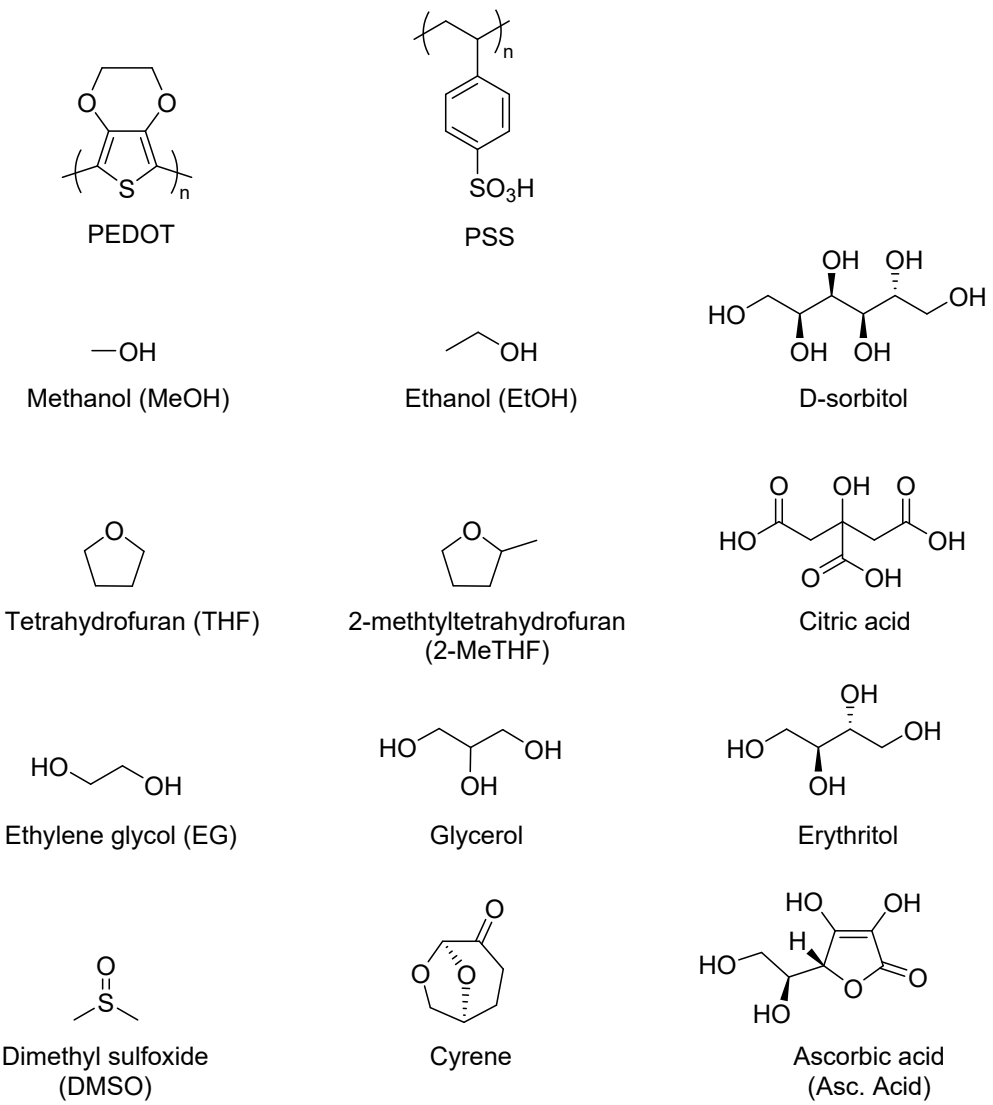

show the change in the measured/calculated parameter relative to the pristine film.

Figure S1. Molecular structures of PEDOT: PSS and used in this study

Table S1. Additive feed stocks

Additive	Feed Stock
Methanol	Natural Gas
Ethylene Glycol	Petroleum
Tetrahydrofuran	Natural gas and petroleum
Dimethyl Sulfoxide	Natural gas
Ethanol	Sugarcane and corncob
Glycerol	Soybean
2-Methyl Tetrahydrofuran	Corncob waste
Cyrene	Cellulose
D-sorbitol	Corn
Citric acid	Molasses and cornstarch
Erythritol	Corn and potato
Ascorbic acid	Corn and potato

Table S2. Film thickness and roughness

Sample	Thickness (µm)	Roughness (nm)
Pristine	10.18 ± 0.13	23.0 ± 0.5
THF	10.66 ± 0.21	19.0 ± 0.6
MeOH	10.30 ± 0.11	11.0 ± 0.6
EG	22.23 ± 0.33	19.0 ± 0.2
DMSO	20.24 ± 0.19	10.0 ± 0.8
2-MeTHF	12.93 ± 0.22	10.1 ± 0.6
EtOH	11.47 ± 0.15	10.0 ± 0.3
Glycerol	29.52 ± 0.05	11.0 ± 0.4
Cyrene	10.33 ± 0.08	10.0 ± 0.7
D-sorbitol	15.00 ± 0.11	12.0 ± 0.7
Citric acid	14.45 ± 0.23	25.0 ± 0.6
Erythritol	22.40 ± 0.20	31.0 ± 0.7
Asc. Acid	11.45 ± 0.16	16.0 ± 0.9

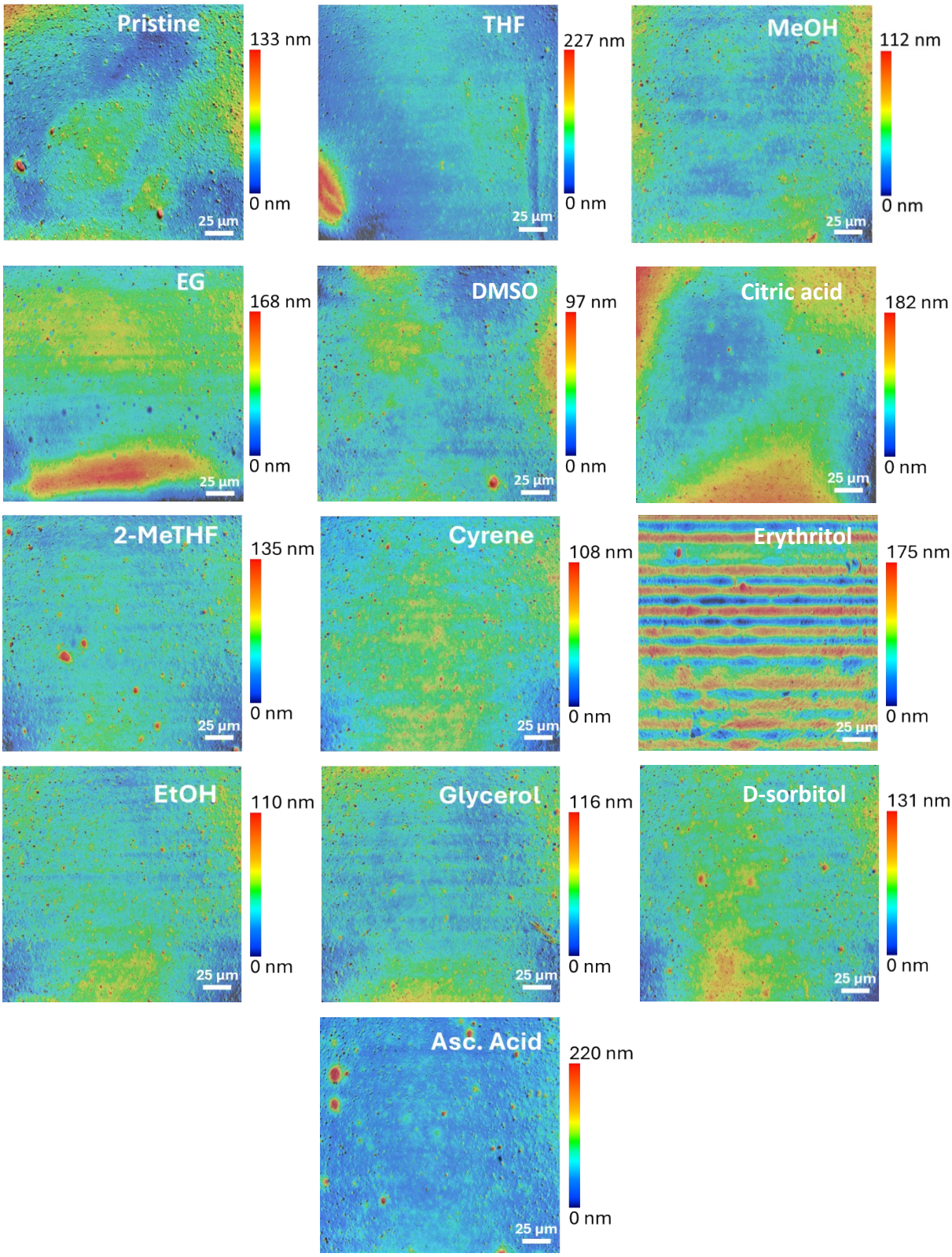

Figure S2. Surface profiles obtained from a laser-confocal microscope (colors represent height)

Table S3. PXRD data for PEDOT: PSS and its additive thin films

Sample		PEDOT -PSS- PEDOT	PEDOT ss	PSS -PEDOT- PSS	PSS ss	PSS π-π	PEDOT π-π	Additive Crystal
Pristine	**2θ**	4.07°	6.65°	ND	13.48°	18.09°	25.68°	ND
	d-spacing	2.17	1.33		0.66	0.49	0.35	
THF	**2θ**	4.31°	7.43°	ND	13.53°	18.32°	26.38°	ND
	d-spacing	2.05	1.19		0.65	0.48	0.34	
MeOH	**2θ**	4.08°	7.27°	ND	13.51°	18.05°	25.80°	ND
	d-spacing	2.16	1.21		0.65	0.49	0.35	
DMSO	**2θ**	3.84°	7.13°	10.22°	ND	18.28°	26.25°	ND
	d-spacing	2.30	1.24	0.86		0.48	0.34	
EG	**2θ**	ND	ND	10.43°	14.36°	18.16°	26.49°	ND
	d-spacing			0.85	0.62	0.49	0.34	
2-MeTHF	**2θ**	4.11°	7.01°	ND	13.56°	17.86°	26.09°	ND
	d-spacing	2.15	1.26		0.65	0.50	0.34	
EtOH	**2θ**	4.09°	7.09°	ND	13.63°	17.72°	25.75°	ND
	d-spacing	2.16	1.23		0.65	0.50	0.35	
Cyrene	**2θ**	4.32°	ND	ND	ND	17.54°	26.14°	ND
	d-spacing	2.04				0.51	0.34	
Glycerol	**2θ**	ND	ND	ND	ND	20.79°	26.31°	ND
	d-spacing					0.43	0.34	
D-sorbitol	**2θ**	ND	ND	ND	ND	18.30°	26.00°	ND
	d-spacing					0.48	0.34	
Citric acid	**2θ**	ND	ND	ND	13.24°	18.09°	26.25°	ND
	d-spacing				0.67	0.49	0.34	
Asc. acid	**2θ**	ND	ND	11.74°	ND	18.06°	26.10°	28.21°
	d-spacing			0.75		0.49	0.34	0.32
Erythritol	**2θ**	ND	ND	10.58°	ND	18.38°	26.04°	14.87°
	d-spacing			0.84		0.48	0.34	0.60

Table S4. Raman peak assignments

Sample	C_β-O-C	C_α-$C_{\alpha'}$	C_β-$C_{\beta'}$	C_α=C_β (Symm.)	C_α=C_β (Asymm.)	C_α=C_β (Asymm.)
Pristine	1120	1261	1369	1442	1537	1571
THF	1120	1261	1369	1438	1537	1567
MeOH	1120	1257	1366	1434	1533	1567
DMSO	1120	1261	1369	1438	1537	1567
EG	1120	1257	1369	1438	1537	1567
2-MeTHF	1120	1261	1369	1438	1537	1567
EtOH	1120	1257	1369	1434	1537	1567
Cyrene	1120	1261	1369	1438	1537	1567
Glycerol	1124	1257	1369	1438	1536	1567
D-sorbitol	1124	1257	1369	1431	1540	1571
Citric Acid	1128	1261	1369	1441	1540	1574
Asc. Acid	1120	1257	1369	1427	1544	1571
Erythritol	1128	1257	1369	1431	1540	1571

-Red shift; -Blue shift; Symmetric stretch (Symm.) and asymmetric stretch (Asymm.)

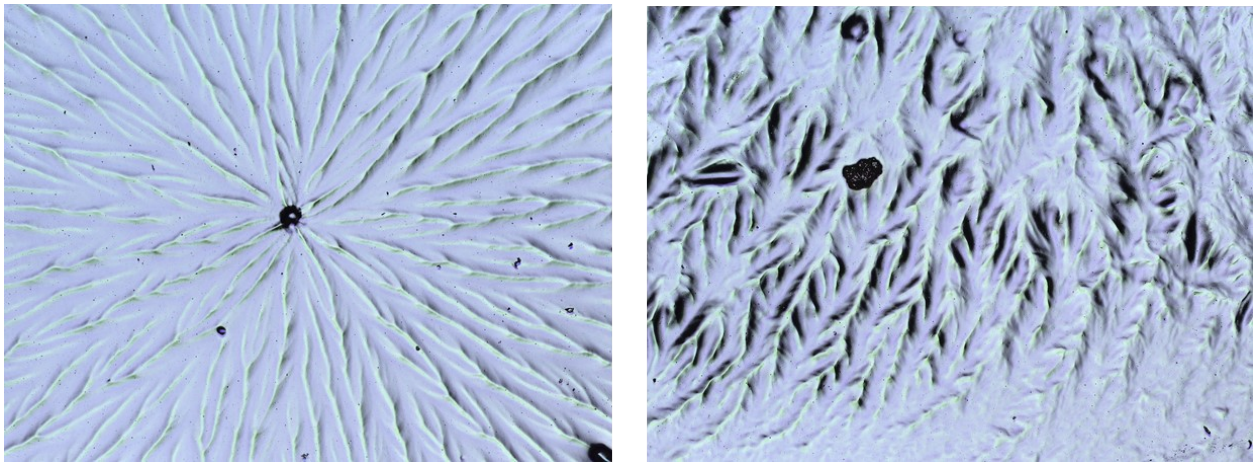

Figure S3. (a) Ascorbic acid crystallite region. (b) Erythritol crystallite region. Images were obtained on a laser-confocal microscope.

Table S5. Compliance coefficients and retardation times used in equation S5

Sample	J_0	J_1	J_2	J_3	τ_1	τ_2	τ_3
Pristine	0.405	0.449	0.576	0.426	1.00	10.0	100
MeOH	0.309	0.473	0.361	0.286	1.00	10.0	100
THF	0.267	0.280	0.322	0.212	1.00	10.0	100
DMSO	0.381	0.572	0.773	0.685	1.00	10.0	100
EG	0.459	0.532	0.705	0.604	1.00	10.0	100
EtOH	0.332	0.389	0.375	0.292	1.00	10.0	100
2-MeTHF	0.302	0.342	0.455	0.269	1.00	10.0	100
Cyrene	0.247	0.279	0.338	0.308	1.00	10.0	100
Glycerol	1.47×10^{-10}	1.79	5.21	0.634	1.00	10.0	100
D-sorbitol	4.28×10^{-10}	1.49	3.81	1.38	1.00	10.0	100
Citric acid	0.512	0.877	2.02	0.0317	1.00	10.0	100
Asc. acid	0.225	0.255	0.390	0.379	1.00	10.0	100
Erythritol	0.681	1.42	1.72	1.01	1.00	10.0	100

Table S6. Modulus coefficients and relaxation times used in equation S6

Sample	μ_∞	μ_1	μ_2	μ_3	λ_1	λ_2	λ_3
Pristine	0.539	1.39	0.400	0.141	2.20	0.163	0.0128
MeOH	0.700	2.04	0.344	0.159	2.61	0.143	0.0124
THF	0.926	2.04	0.582	0.203	2.12	0.155	0.0123
DMSO	0.415	1.78	0.320	0.113	2.95	0.166	0.0129
EG	0.435	1.25	0.355	0.136	2.26	0.167	0.0133
EtOH	0.721	1.71	0.409	0.173	2.24	0.149	0.0125
2-MeTHF	0.731	1.88	0.539	0.159	2.22	0.166	0.0123
Cyrene	0.854	2.30	0.637	0.268	2.218	0.160	0.0134
Glycerol	0.131	6.81×10^9	0.202	9.90×10^{-3}	1.58×10^{10}	0.304	0.0108
D-sorbitol	0.150	2.34×10^9	0.249	0.0320	4.40×10^9	0.287	0.0124
Citric acid	0.291	1.36	0.304	2.40×10^{-3}	2.98	0.223	0.0101
Asc. acid	0.801	2.57	0.786	0.300	2.25	0.176	0.0140
Erythritol	0.207	1.04	0.168	0.0479	3.27	0.174	0.0125

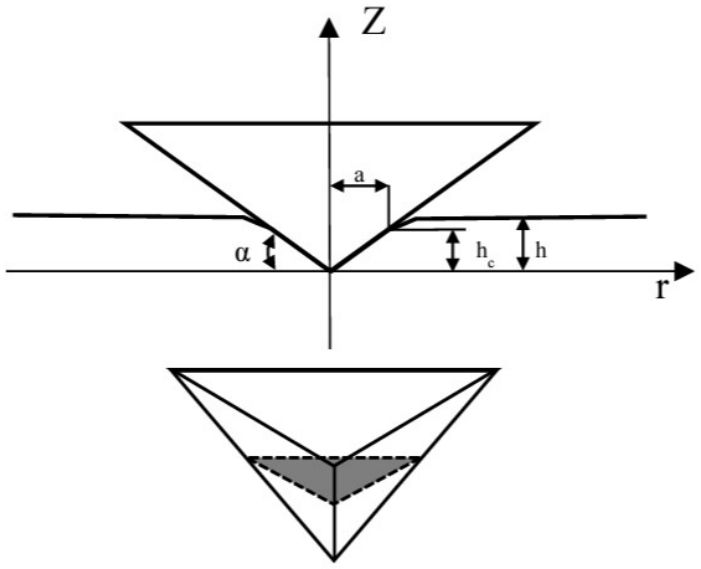

Figure S4. Indentation parameters and Berkovich indenter tip geometry

Table S7. PEDOT: PSS interfacial shear strength and relative change

Sample	Interfacial Shear Strength (kPa)	Percent Change (%)
Pristine	19.4 ± 0.6	NA
2-MeTHF	23.1 ± 1.2	+19.1
EG	23.7 ± 0.9	+22.2
Cyrene	25.0 ± 1.4	+28.9
EtOH	25.8 ± 1.2	+33.0
THF	27.3 ± 0.4	+40.7
Erythritol	27.6 ± 0.8	+42.3
Glycerol	28.0 ± 0.9	+44.3
MeOH	28.1 ± 1.4	+44.8
Asc. Acid	28.1 ± 1.1	+44.8
DMSO	29.5 ± 1.4	+52.1
D-sorbitol	31.7 ± 2.1	+63.4
Citric Acid	33.3 ± 1.0	+71.6

Standard deviation was calculated from three tests per sample.

Table S8. PEDOT: PSS contact angles on PET

Sample	Contact Angle (°)	Percent Change (%)
Pristine	42.6 ± 1.1	NA
2-MeTHF	34.6 ± 1.1	-18.8
EG	35.3 ± 0.7	-17.1
Cyrene	31.0 ± 1.1	-27.2
MeOH	29.8 ± 0.7	-30.0
EtOH	32.2 ± 1.0	-24.4
THF	31.7 ± 1.3	-25.6
Asc. Acid	29.8 ± 1.6	-30.0
Glycerol	31.6 ± 0.9	-25.8

DMSO	30.8 ± 1.6	-27.7
Erythritol	31.7 ± 1.5	-25.6
D-sorbitol	29.6 ± 0.8	-30.5
Citric Acid	29.6 ± 1.3	-30.5

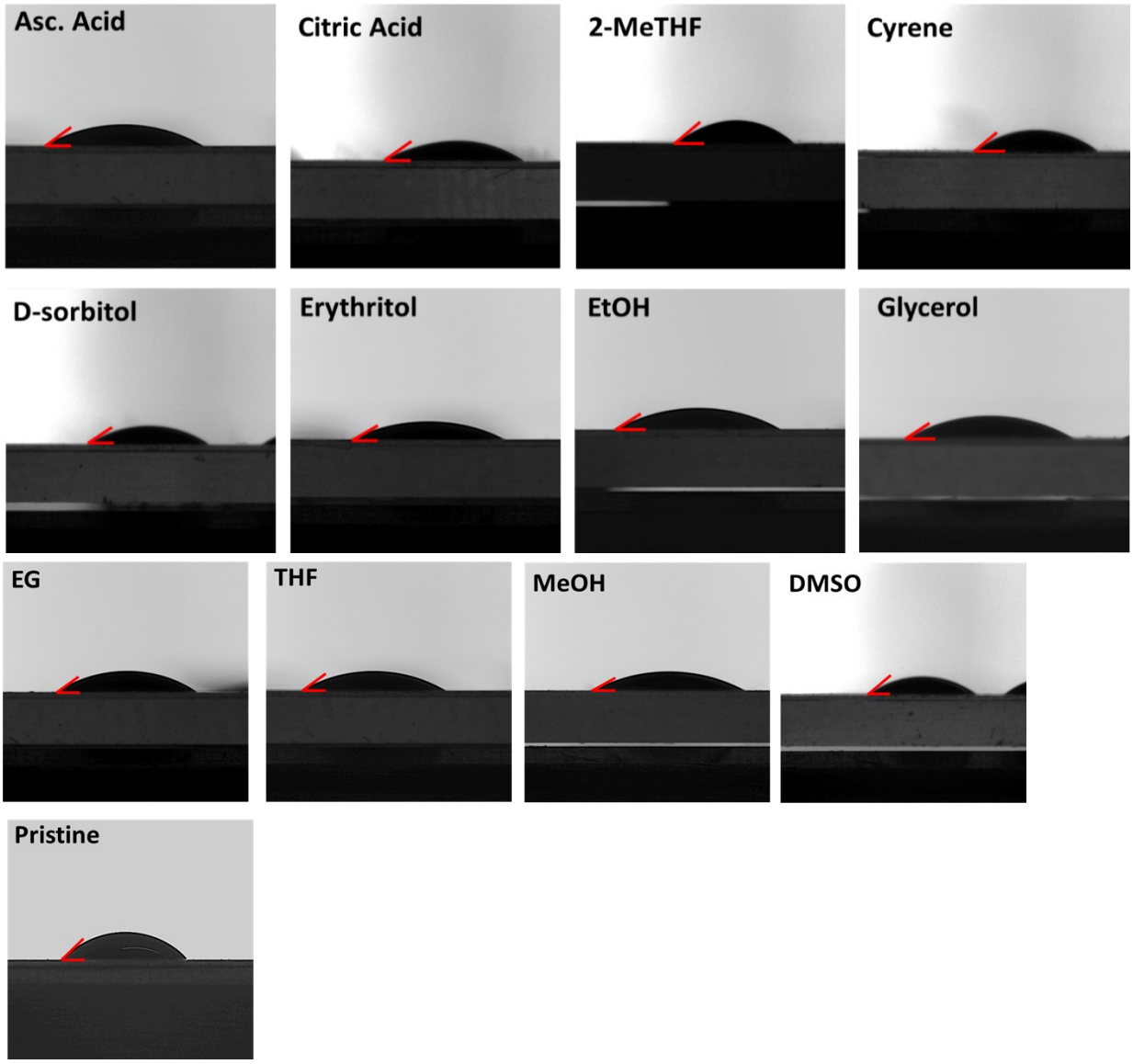

Figure S5. PEDOT: PSS contact angle images

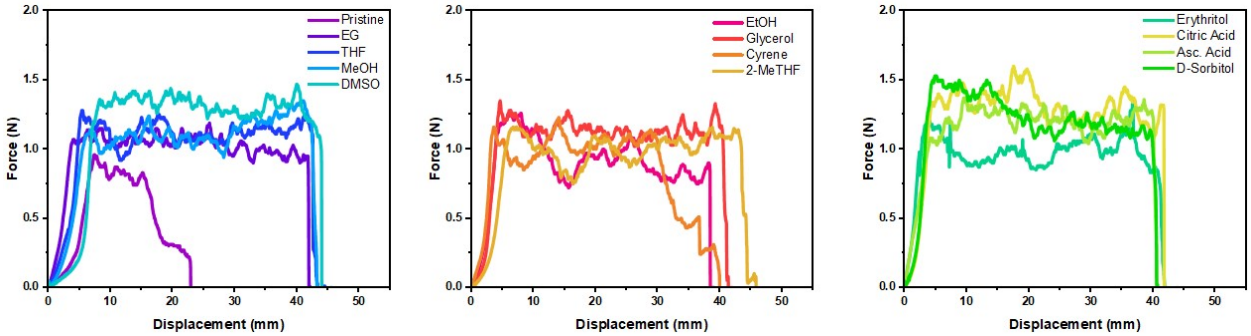

Figure S6. Force-displacement curves for 180° peel tests

Table S9: Conductivity measurement data for all PEDOT: PSS film samples

	R1	R2	R3	R4	R5	Ravg	Rstdev	Error	ρ	σavg	t	t(cm)
Name	Ω	Ω	Ω	Ω	Ω	Ω	Ω	Ω	Ωcm	S/cm		
Pristine	2770	2620	2510	2730	2180	2633.333	77.67453	2.949666	1.215004	0.823043	10.18	0.000102
THF	1010	1380	1310	1030	1530	1233.333	112.3981	9.11336	0.595884	1.678179	10.66	0.000107
2-MeTHF	1205	1477	1411	1511	1652	1364.333	50.84617	3.726815	0.799545	1.250711	12.93	0.000129
EtOH	958	876	1110	1212	912	981.3333	41.1015	4.188332	0.510157	1.96018	11.47	0.000115
MeOH	675	854	737	813	725	755.3333	59.3661	7.859589	0.352614	2.83596	10.3	0.000103
Erythritol	264	336	425	346	338	341.8	5.291503	1.548128	0.347012	2.881747	22.4	0.000224
Asc. Acid	825	1050	969	1100	1030	948	61.61006	6.498952	0.491969	2.032648	11.45	0.000115
D-Sorbitol	30.8	27.5	26.2	20.6	27.7	28.16667	0.814453	2.891548	0.019149	52.22149	15	0.00015
Cyrene	10.6	10.5	8.35	8.58	10.5	9.816667	0.057735	0.588133	0.004596	217.5763	10.33	0.000103
Glycerol	4.95	4.74	3.05	4.16	0.5	3.48	0.409186	11.75822	0.004656	214.7733	29.52	0.000295
DMSO	4.32	4.06	4.25	3.36	3.26	4.21	0.134536	3.195635	0.003862	258.9306	20.24	0.000202
Citric Acid	2.955	3.386	2.304	3.678	3.083	2.881667	0.221342	7.681045	0.001887	529.8639	14.45	0.000145
EG	2.38	2.58	2.2	1.989	2.213	2.386667	0.100381	4.205905	0.002405	415.8577	22.23	0.000222

Table S10: Comparative summary of different PEDOT: PSS and its additive samples.

Sample	**Conductivity (S/cm)**	**Young's Modulus (GPa)**	**Interfacial Shear Strength to PET (kPa)**
Pristine	0.82 ± 0.02	1.434 ± 0.019	19.4±0.59
2-MeTHF	1.25 ± 0.05	1.945 ± 0.101	23.1±1.23
THF	1.68 ± 0.15	2.462 ± 0.039	27.3±0.4
EtOH	1.96 ± 0.08	1.918 ± 0.048	25.8±1.24
Asc. Acid	2.03 ± 0.13	2.131 ± 0.020	28.1±1.09
MeOH	2.84 ± 0.22	1.861 ± 0.170	28.1±1.40
Erythritol	2.88 ± 0.04	0.551 ± 0.015	27.9±0.66
D-sorbitol	52.2 ± 1.50	0.398 ± 0.005	31.7±2.1
Glycerol	176 ± 7.35	0.348 ± 0.034	28±0.91
Cyrene	218 ± 30.8	2.271 ± 0.035	25±1.44
DMSO	259 ± 8.00	1.309 ± 0.017	29.5±1.40
EG	416 ± 14.4	1.156 ± 0.012	23.7±0.9
Citric Acid	530 ± 48.8	0.773 ± 0.020	33.3±1

References

1. Lu, H. W., B.; Huang, J. MA.; Viswanathan, H., Measurement of Creep Compliance of Solid Polymers by Nanoindentation. *Mechanics of Time-Dependent Materials* **2002,** *7*, 189-207.

2. Lang, U.; Naujoks, N.; Dual, J., Mechanical characterization of PEDOT:PSS thin films. *Synthetic Metals* **2009,** *159* (5-6), 473-479.

3. Greco, F.; Zucca, A.; Taccola, S.; Menciassi, A.; Fujie, T.; Haniuda, H.; Takeoka, S.; Dario, P.; Mattoli, V., Ultra-thin conductive free-standing PEDOT/PSS nanofilms. *Soft Matter* **2011,** *7* (22).

4. Luk-Cyr, J.; Crochon, T.; Li, C.; Lévesque, M., Interconversion of linearly viscoelastic material functions expressed as Prony series: a closure. *Mechanics of Time-Dependent Materials* **2012,** *17* (1), 53-82.

5. F. Greco, A. Zucca, S. Taccola, A. Menciassi, T. Fujie, H. Haniuda, S. Takeoka, P. Dario and V. Mattoli, *Soft Matter*, **2011**, *7*, 10642–10650.